General approach for quantitative description of the Background Voltammograms

Nigmatullin RR[1], Budnikov HC[2], Sidelnikov AV[3] and Elza I Maksyutova[3]*

[1]*Radioelectronic and Informative-Measurements Techniques Department, Kazan National Research Technical University (KNRTU-KAI),
Kazan, Russia*
[2]*Institute of Chemistry, Kazan Federal University (KFU), Kazan, Russia*
[3]*Chemistry Department, Bashkir State University (BSU), Ufa, Russia*

Article Info

*Corresponding author:
Elza I Maksyutova
Department of Chemistry
Bashkir State University (BSU)
Ufa, Russia
Email: artsid2000@gmail.com,
elzesha@gmail.com

Abstract

Based on the hypothesis related to fractal structure of electrode one can develop the quantitative theory for description of the measured voltammograms (VAGs). We suppose that at least two percolation channels take part in the process of its formation. One channel can be associated with the fractal structure of electrodes while the second one can be related to the heterogeneous structure of the double electric layer. Based on the obtained fitting function that follows from the suggested theory it becomes possible to differentiate the state of two measured electrodes (with regeneration or without application of this procedure). This result obtained directly from the measured data can find a wide application in electrochemistry for analysis of other VAGs, especially in detection of possible traces of substances that take place in chemical reactions in the vicinity of heterogeneous electrodes.

Keywords: Electrochemistry; Quantitative Fractal Theory; Regenerated/No Regenerated Electrodes; Self-Similar Voltammograms; Traces Detection.

List of abbreviations: BLC - bell-like curve, DEL - double electric layer, GCE - the glassy carbon electrode, ECs - the eigen-coordinates method, LLSM - the linear least square method, PD - potential distribution, VAG(s) - voltammogram(s).

Introduction and Formulation of the Problem

As it is known for detection of the limit of sensitivity of the presence of a substance by electrochemical methods a researcher uses the series of measurements in the presence of analyte (i.e. a blank experiment) or the background electrolyte. Detection of this signal determines the minimal concentration of the electrolyte in the analyzed object [1]. Detection of this signal gives a possibility (with some value of probability) to extract a useful signal among random factors (noises) and based on the ratio signal/noise (S/N) to evaluate the desired limit of detection. This limit can be evaluated in accordance with standard deviation (dispersion of the background signal) using the ratio $3s_{bg}/b$, where b determines the sensor sensitivity coefficient. The uncontrollable factors (noises) can have different origins. It can be suppressed by chemical/instrumental methods [2,3] or based on some mathematical methods, for example, with the help of projection method suggested by chemometrics [4]. The complete elimination of the background is impossible. Especially, it creates a big problem in interpretation of complex multi-parametric data in the presence of multisensors. To this problem one can refer, for example, the VAGs associated with electronic "tongue" [5].

For the increasing of electrochemical resolution many methods were suggested and their descriptions one can find in paper [6]. However, even in the conditions of the well-resolved peaks, the measured VAGs contain the background current component (for

Madridge J Anal Sci Instrum.
ISSN: 2638-1532

Volume 2 • Issue 1 • 1000110

47

example, capacity current), which strongly distorts the measured VAG, especially at small electrolyte concentrations. This problem complicates the data decoding and decreases the sensitivity and accuracy of the electrochemical analysis in detection of possible traces of the presence substance. These existing problems are described in papers [3,6]. The mathematical modeling of the voltammetric behavior on different types of electrodes is discussed in [7]. But it is necessary to note that many leading researches (Compton et al) demonstrate the forms of the VAGs for electrodes having large surface and for relatively large concentrations of depolarizer (at large values of the faraday currents) and, naturally, the "background" problems are skipped and not discussed properly [7].

In the conditions of multivariate study the synergetic effects of the present components in formation of the double electric layer (DEL) strongly distort the measured curves [8,9]. We want to stress also that approach based on the subtraction of the signals in the systems of the electronic tongue type becomes useless [10,11].

It is obvious that new approaches for decoding and mathematical description of the VAGs are necessary. They should take into account the factors that influence on the dispersion of the background signals in all possible range of potential created by the used sensor. In this aspect a certain interest can be referred to approaches associated with electrochemical behavior of electroactive particles on different electrodes based on the ideas of fractal geometry [12-17]. It is well known that electrochemical activity as response of the electrode varies over its surface. One can propose some cases of such typical phenomena:

a) partially blocked electrode,

b) composite electrode (made of composite material with nanoparticles),

c) chemically modified electrode (especially with catalytic active particles),

d) Screen printed partially blocked electrode with random particles of various forms on the surface.

In all these cases a chaotic distribution of particles is observed. Partially blocked electrode is used for ordinary case especially when a macro electrode covered with inert particles of a material is different to that of the underlying electrode surface. These particles can block the diffusional paths of the electroactive species to the electrode surface. To be true, this conclusion is only correct if both zones of the electrodes - blocked and exposed - are of macro size. If they are of micron-sized dimensions then the voltammetric response is much more difficult to predict [7]. This brief review of the present situation allows formulating the problem that can be considered in this paper.

The authors suggest an original approach to description of the real background electrolyte based on the confirmed real data. This approach based on the fractal theory allows to describe quantitatively the behavior of the measured VAGs associated with real electrolyte in two conditions: (a) when the sensor was regenerated; (b) when the sensor becomes idle and was not subjected to the regeneration procedure.

For more accurate detection of these different states it would be desirable to suggest the analytical form of the given voltammogram (VAG) or the fitting function. Based on the preliminary results obtained earlier in [18] in this paper we give some arguments for justification of the desired dependence of the function $J(U)$. With the help of the eigen-coordinates method (developed earlier by one of the authors (RRN)) in [19] we proved that the function $J(U)$ is described by a linear combination of the power-law exponents with log-periodic corrections. As it follows from the general theory described below the desired fitting function based on the fractal structure of the medium (one can imply the surrounding DEL) and heterogeneous electrodes themselves can be written as

$$J(z) = \sum_{l=1}^{L} z^{\nu_l} \Pr_l(\ln z), \ \Pr_l(\ln z \pm \ln \xi) = \Pr_l(\ln z), \ z = U/U_0$$

$$\Pr_l(\ln z) = A_0^{(l)} + \sum_{k=1}^{K \gg 1} \left[Ac_k^{(l)} \cos\left(2\pi k \frac{\ln z}{\ln \xi}\right) + As_k^{(l)} \sin\left(2\pi k \frac{\ln z}{\ln \xi}\right) \right]. \tag{1}$$

The number of the power-law exponents n_l ($l = 1,2,...,L$) for description of the given VAG and the value of the final mode K should be sufficient for keeping the value of the relative fitting error less than 5%-7%. The parameter z coincides with the dimensionless potential U_{sh}/U_0 shifted to positive region ($z > 0$). The power-law exponents n_l ($l = 1, 2,..., L$) are real but the complex-conjugated parts are appeared from the log-periodic functions $\Pr_l(\ln z)$. For explanation and justification of expression (1) chosen as the basic fitting function one can suggest rather general theory based on idea of formation of some self-similar percolation channels connecting the total current under the applied potential. This theory justifies expression (1) chosen as the fitting function and naturally explains the appearance of the complex-conjugated power-law exponents.

The content of the paper is organized as follows. In the second section we describe the experimental details. In the third chapter we suggest the general theory that explains expression (1) and its possible modifications. In the fourth section the desired algorithm for the fitting of the background currents for different electrodes is described. In the final section we discuss the obtained results and speculate about the physical/chemical meaning of the suggested fitting function.

Experimental

Reagents and the used equipment

All voltammetric measurements were performed with the help of three-electrode scheme and the usage of voltammetric analyzer IVA-5 (Yekaterinburg, Russia). The glassy carbon electrode (GCE) was used as the working electrode. The glassy carbon pivot and chloride-silver Ag/AgCl (3.5 M KCl) electrode were used as an auxiliary electrode and comparison electrode, correspondingly. Voltammetric measurements were performed in the potential range from 0.0 up to -1.5 V in the given cycling regime. For the cleaning of the electrode surface at mechanical regeneration the standard GOI polishing paste was used.

Madridge J Anal Sci Instrum.
ISSN: 2638-1532

Volume 2 • Issue 1 • 1000110

48

Voltammetric measurements

In the electrochemical cell 10 ml of the standard solution of 0.1 M KCl was placed. Each experiment includes the electrochemical cleaning of the standard GCE during 30 sec at the applied potential 0.4 V. The cyclic VAGs were registered in the potential range 0.0 - (-1.5) V with the scanning rate 0.1 V/sec. All measurements were performed at room temperature (21-23°C). We obtained two types of VAGs: the first type - the measured data for electrodes without regeneration (electrodes were kept in the measured cell during the whole period of measurements). The second type of VAGs was obtained with the usage of regeneration procedure, when the surface of electrodes was polished on the smooth paper by a special GOI polishing paste having small grains. For verification of stability of the measurements each cycle of experiment was repeated 100 times.

Results and Discussion

The general theory for quantitative description of the desired VAG

For explanation and justification of the chosen curve (1) we put forward the following arguments. Let the function $f(zx^n)$ describes the distribution of the dimensionless potential $z=U/U_0$ over some fractal electrode. The arising current $J(z)$ evoked by the applied potential is distributed over percolation regions and the distribution of these regions has a fractal (scaling) structure. Mathematically this supposition will be expressed in the form of the sum

$$J_l(z) = R_l \sum_{n=-N}^{N} b_l^n \cdot f_l(z\xi^n) \tag{2}$$

Here the value $R_l b_l^n$ determines the percolation region that can coincide with volume ($d_E=3$), surface ($d_E=2$) or conducting line ($d_E=1$). The function $f_l(z\xi^n)$ determines the distribution function of the potentials that can be specific for each l-th "channel" of the type (2) that provides the percolation process of the total current from one electrode to another one. For any heterogeneous structure that constitutes a possible fractal structure of the used electrodes and percolation regions of the conducting "surrounding" (including also the DEL) we suppose that all conducting channels form an additive combination of currents that can connect two or more electrodes with each other. So, one can write the following expression for the total current as

$$J_{tot}(z) = \sum_{l=1}^{L} J_l(z) = \sum_{l=1}^{L} R_l \sum_{n=-N}^{N} b_l^n f_l(z\xi^n) \tag{3}$$

We suppose also that the function describing the potential distribution (PD) for each microscopic current $f_l(z\xi^n)$ has the following asymptotic behavior at small and large values of N

For $z << 1$

$$f_l(z) = c_{l,0}z + c_{l,1}z^2 + ... \tag{4a}$$

For z >> 1

$$f_l(z) = \frac{B_{l,0}}{z} e^{-\lambda_{l,0}z} + \frac{B_{l,1}}{z^2} e^{-2\lambda_{l,0}z} + ... \tag{4b}$$

If the values of these functions $f_l(z\xi^n)$ ($l = 1,2,...,L$) are small for large and small values of z then one can show [20-22] that the fractal sum (2) can be reduced to the simplified functional equation of the type

$$J_l(z\xi) \cong \frac{1}{b_l} J_l(z), \tag{5}$$

For any combination of parameters b_l, x. It implies that asymptotic influence of the PD function becomes small ($\left| b_k^N f(z\xi^{N+1}), b_k^{-N-1} f(z\xi^{-N}) \right| < A_0 < 1$ in the ends of a fractal region [20]. The solution of the functional equation (5) is expressed in the form

$$J_l(z) = \left(\frac{1}{b_l}\right)^{\frac{\ln(z)}{\ln(\xi)}} \Pr_l(\ln(z)) = z^{\nu_l} \Pr_l(\ln(z)), \quad v_l = \frac{\ln(1/b_l)}{\ln(\xi)}. \tag{6}$$

The log-periodic function is defined by expression (1). Let us suppose that we have at least two "channels" of the type (2) and the total percolation process is expressed as

$$J_{tot}(z) = J_1(z) + J_2(z)$$
$$J_{tot}(z\xi) = \frac{1}{b_1} J_1(z) + \frac{1}{b_2} J_2(z)$$
$$J_{tot}(z\xi^2) = \frac{1}{(b_1)^2} J_1(z) + \frac{1}{(b_2)^2} J_2(z) \tag{7}$$

Excluding two channels $J_{1,2}(z)$ from the first two lines and inserting them to the final line we obtain the following functional equation for the total current

$$J_{tot}(z\xi^2) = a_1 J_{tot}(z\xi) + a_0 J_{tot}(z), \tag{8}$$

where

$$a_1 = (\kappa_1 + \kappa_2), \quad a_0 = -\kappa_1 \cdot \kappa_2, \quad \kappa_{1,2} = (b_{1,2})^{-1} \tag{9}$$

In paper [22] it was shown that this functional equation has the following solution

$$J_{tot}(z) = \sum_{l=1}^{2} \kappa_l^{\ln(z)/\ln\xi} \Pr_l(\ln z) = \sum_{l=1}^{2} z^{\nu_l} \Pr_l(\ln z), \tag{10}$$

Using the mathematical induction method one can show that this result can be generalized for "L" conducting channels. For this case we obtain

Madridge J Anal Sci Instrum.
ISSN: 2638-1532

Volume 2 • Issue 1 • 1000110

49

$$J_{tot}\left(z\xi^L\right) = a_{L-1}J_{tot}\left(z\xi^{L-1}\right)+...+a_0J_{tot}\left(z\right),$$

$$a_{L-1}=\left(-1\right)^{L-1}\left(\kappa_1+\kappa_2+...+\kappa_L\right),$$

$$a_{L-2}=\left(-1\right)^{L-2}\left(\kappa_1\kappa_2+\kappa_1\kappa_3+...+\kappa_{L-1}\kappa_L\right) \quad (11)$$

.

.

$$a_0 = \kappa_1 \cdot \kappa_2 ... \cdot \kappa_L$$

As for the case $L = 2$ the desired roots k_l are related to the scaling parameters b_l by means of simple relationships $k_l = 1/b_l$ ($l = 1,2,...,L$). The solution of the functional equation (11) has the following form [22]

$$J_{tot}(z) = \sum_{l=1}^{L} \kappa_l^{\ln(z)/\ln\xi} \operatorname{Pr}_l(\ln z) = \sum_{l=1}^{L} z^{\nu_l} \operatorname{Pr}_l(\ln z),$$

$$\nu_l = \frac{\ln(\kappa_l)}{\ln\left(\xi\right)}. \quad (12)$$

In order to minimize the number of the fitting parameters we consider in detail the case $L=2$. The fitting function that can describe the desired VAG can be rewritten in the form

$$J_{tot}(z) = E_1\kappa_1^{\ln z/\ln\xi} + \sum_{k=1}^{K}\left[Ac_k^{(1)}yc_k^{(1)} + As_k^{(1)}ys_k^{(1)}\right]$$

$$+E_2\kappa_2^{\ln z/\ln\xi} + \sum_{q=1}^{Q}\left[Ac_q^{(2)}yc_q^{(2)} + As_q^{(2)}ys_q^{(2)}\right] \quad (13)$$

$$yc_k^{(1,2)} = \kappa_{1,2}^{\ln z/\ln\xi}\cos\left(2\pi k\frac{\ln z}{\ln\xi}\right), \quad ys_k^{(1,2)} = \kappa_{1,2}^{\ln z/\ln\xi}\sin\left(2\pi k\frac{\ln z}{\ln\xi}\right).$$

In order to reduce number of the fitting parameters in expression (13) we suppose that two channels involved in the percolation process have equal contributions ($K = Q$). For this case the function (13) admits further simplification and finally for the case $L=2$ we obtain the following fitting function

$$J_{tot}(\ln z) = E_0\left(\kappa_1^{\ln z/\ln\xi} + \kappa_2^{\ln z/\ln\xi}\right) + \sum_{k=1}^{K}\left[Ac_k^{(1)}yc_k^{(1)} + As_k^{(1)}ys_k^{(1)}\right]$$

$$+\sum_{k=1}^{K}\left[Ac_k^{(2)}yc_k^{(2)} + As_k^{(2)}ys_k^{(2)}\right], \quad (14)$$

$$yc_k^{(1,2)} = \kappa_{1,2}^{\ln z/\ln\xi}\cos\left(2\pi k\frac{\ln z}{\ln\xi}\right), \quad ys_k^{(1,2)} = \kappa_{1,2}^{\ln z/\ln\xi}\sin\left(2\pi k\frac{\ln z}{\ln\xi}\right).$$

In the next section we show *how* to calculate the desired parameters $k_{1,2}$ and nonlinear fitting parameters as lnx and K. Obviously, the common scaling parameter lnx that enters in the general expressions (12-14) should be interpreted in the mean value sense. This simplification and selection the common value for all possible channels is explained in the Mathematical Appendix.

Some peculiarities of the fitting of expression (14) to real data

In this fitting function we have 4 nonlinear parameters $k_{1,2}$, lnx and K. Other fitting parameters as $E_0, Ac_k^{(1,2)}, As_k^{(1,2)}$ equaled to $4K+1$ are found by the LLSM. The value of the desired x is located in the interval

$$0 < \xi < \xi^2 \quad (\xi > 1), \quad (15)$$

While the final value of K is calculated from the condition that the value of the fitting error should not exceed 5-7% for simple case. This value is calculated as

$$\operatorname{Re}lErr(\%) = \left|\frac{stdev(y(z) - J_{tot}(z,\vec{v}))}{mean(y(z))}\right| \cdot 100\% \quad (16)$$

Where the fitting function $J_{tot}(z,\vec{v})$ coincides with the simplified expression (14), the fitting vector $\vec{v} \equiv v(\ln\xi, K)$ and $y(z)$ coincides with mean measurement VAG. The evaluation of this mean measurement from the given set of data is explained in the next section. We should stress here that in the case of negative values of k that can enter in the fitting function (14) the corresponding expression should be replaced as

$$\left(-\kappa\right)^{\ln z/\ln\xi} \Rightarrow \left(\left|\kappa\right|\right)^{\ln z/\ln\xi}\cos\left(\pi\frac{\ln z}{\ln\xi}\right) \quad (17)$$

The Description of the Data Processing Procedure

The basic problem that can be solved in the frame of the suggested theory is formulated as follows: is it possible "to notice" the difference between non-regenerated and regenerated electrodes and express their differences quantitatively? All treatment procedure can be divided on three basic stages that can be recommended as a common procedure for all similar measurements, as well.

Stage 1. Reduction to Three Mean Measurements.

We show this procedure for electrode without regeneration. It is also explained by the figures given below. The same procedure will be applied to analysis of the VAGs with regeneration. The initial hysteresis (cycle) of the measured function $J(U)$ for electrodes without regeneration is shown in Fig.1. Accordingly, the VAGs corresponding to the regeneration procedure were shown in Fig.2.
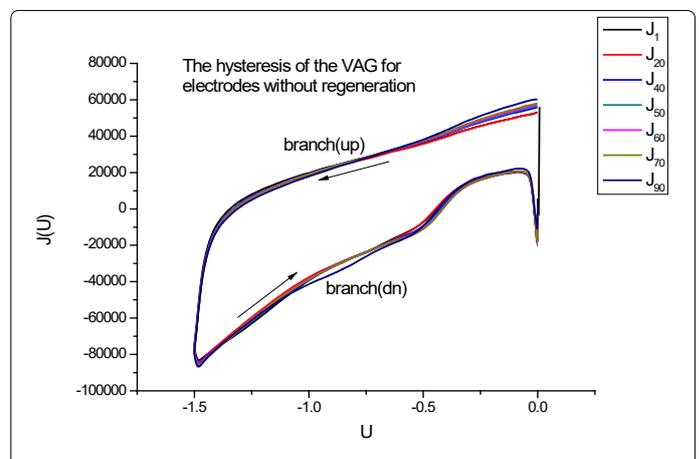

Figure 1. The hysteresis (cycling) of the VAG corresponding to electrodes used without process of regeneration.

For further analysis we divide the hysteresis on two branches (up and down) correspondingly and consider them separately.

Madridge J Anal Sci Instrum.
ISSN: 2638-1532
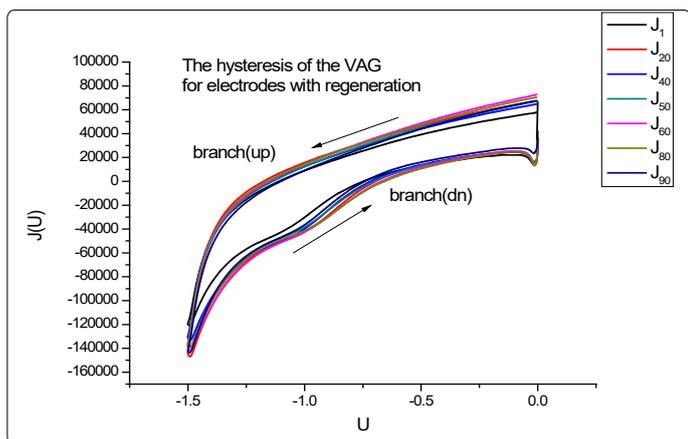
Volume 2 • Issue 1 • 1000110

50

Figure 2. The hysteresis of the VAG corresponding to electrodes subjected to the regeneration procedure.

One can notice visually the difference between these VAGs but the basic aim is to find the fitting function for these curves and then "read" and compare them quantitatively.

The basic aim of this stage is to receive the averaged VAGs that can be prepared for the fitting procedure with the function (14). In order to realize the correct averaging procedure we consider the branches (up and down) forming the initial hysteresis separately. We consider the distribution of the slopes with respect to mean measurement

$$Sl_m = slope(\langle J \rangle, J_m) \equiv \frac{\left(J_m \cdot \langle J \rangle \right)}{\left(\langle J \rangle \cdot \langle J \rangle \right)},$$

$$\langle J \rangle = \left(\frac{1}{M} \right) \sum_{m=1}^{M} J_m, \quad \left(A \cdot B \right) = \sum_{j=1}^{N} A_j B_j. \qquad (18)$$

Here $M=100$ coincides with the total number of measurements for the given background. The sufficiently large of repetitions ($50 < M < 100$) of the same electrochemical background are necessary for analysis of statistical peculiarities and the influence of external conditions that will take place during the whole experiment. The parenthesis in (18) determines the scalar product between two functions having $j=1,2,...,N$ measured data points. If we construct the plot Sl_m with respect to successive measurement m and then rearrange all measurements in the descending order $SL_1 > SL_2 > ... > SL_M$, then all measurements can be divided in three groups. The "up" group has the slopes located in the interval $(1+D_{up}, SL_1)$; the mean group (denoted by "mn") with the slopes in $(1-D_{dn}, 1+D_{up})$; the down group (denoted by "dn") with the slopes in $(1-D_{dn}, SL_M)$. The values $D_{up,dn}$ are chosen for each set of the VAG measurements separately. In our case we chose the conventional "3sigma" criterion and put

$\Delta_{up} = \frac{Sl_1 - 1}{3}, \Delta_{dn} = \frac{1 - Sl_M}{3}$. This curve has a great importance and reflects the quality of the realized successive measurements and the used equipment. Different cases for 4 different branches and two types of electrodes are shown on Figs. 3(a, b, c, d), correspondingly. The bell-like curve (BLC) (that can be fitted with the help of four fitting parameters α, β, A, B) is obtained after elimination of the corresponding mean value and subsequent integration can be described by the non-

normalized beta-function

$$Bd(m; \alpha, \beta, A, B) = A(m)^{\alpha} \left(M - 1 - m \right)^{\beta} + B, \qquad (19)$$

and reflects the quality of the realized measurements. This presentation is very convenient and contains additional information about the process of measurement that before was not taken into account. The straight line (it can have a slope not coinciding with horizontal line) divides all measurements in three groups: (a) the beginning point of a BLC up to the first intersection point determines the number Nup of measurements $J_m^{(up)}(x)$ ($m=1,2,..., Nup$) entering in the "up" group and is characterized by the mean $Yup(x)$ curve; (b) the region between the two intersection points determines the number Nmn of measurements $J_m^{(mn)}(x)$ ($m=1,2,...,Nmn$) in the "mn" group with slope close to one and characterized by the set of measurements forming the mean curve $Ymn(x)$ and, finally, (c) the rest of the measurements Ndn in the "dn" group is covered by the curve $Ydn(x)$. If the number of measurements $Nmn > Nup+Ndn$ then this cycle of measurements is characterized as "good" (stable), in the case when $Nmn \gg Ndn \gg Nup$ the measurements (and the corresponding equipment) are characterized as "acceptable", and the case when $Nmn < Nup+ Ndn$ is characterized as "bad" (very unstable). Quantitatively, all three cases can be characterized by the ratio

$$Rt = \left(\frac{Nmn}{Nup + Ndn + Nmn} \right) \cdot 100\% = \left(\frac{Nmn}{M} \right) \cdot 100\% \qquad (20)$$

In the last expression (4), M determines the total number of measurements. Based on this ratio one can determine easily three classes of measurements: "good" when $60\% < Rt < 100\%$, "acceptable" when $30\% < Rt < 60\%$, and "bad" when $0 < Rt < 30\%$. This preliminary analysis is supported by Figs. 3(a, b, c, d) for four branches of the measurements with/without electrodes regeneration.
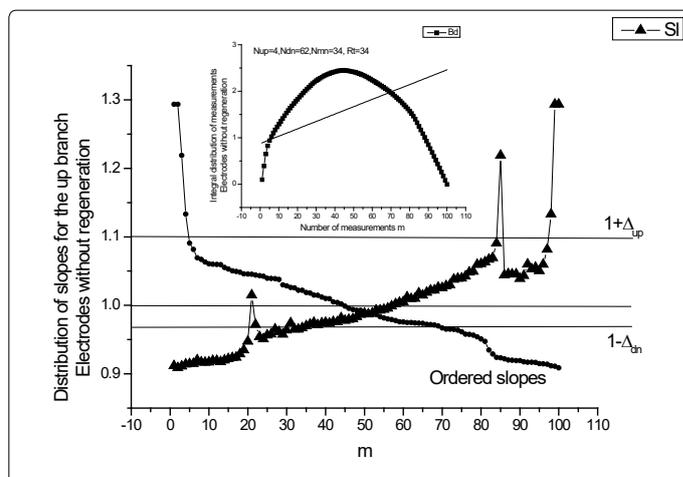

Figure 3a. The distributions of the slopes corresponding to the "up" branches of experiments without regeneration. Number of measurements participating in the averaging procedure and satisfying to the condition $((Nup=4)+(Ndn=62)+(Nmn=34)=(M=100))$ and the parameter Rt from (4) are shown in the small figure above.
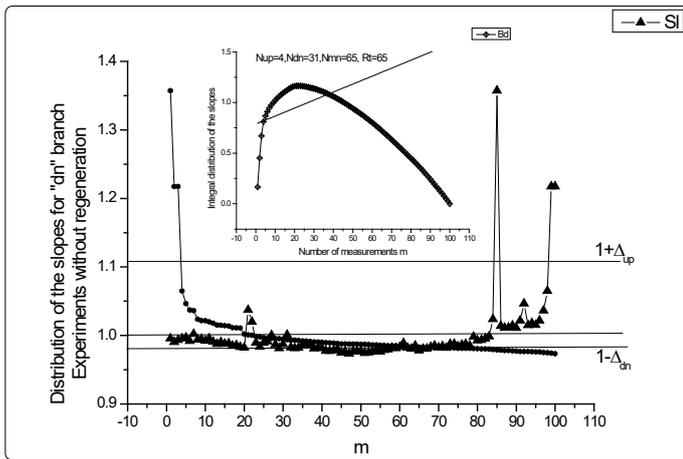
Figure 3b. The distributions of the slopes corresponding to the "dn" branches of experiments without regeneration. Number of measurements participating in the averaging procedure and satisfying to the condition
((Nup=4)+(Ndn=31)+(Nmn=65)=(M=100)) and the parameter Rt=65 from (4) are shown in the small figure above.
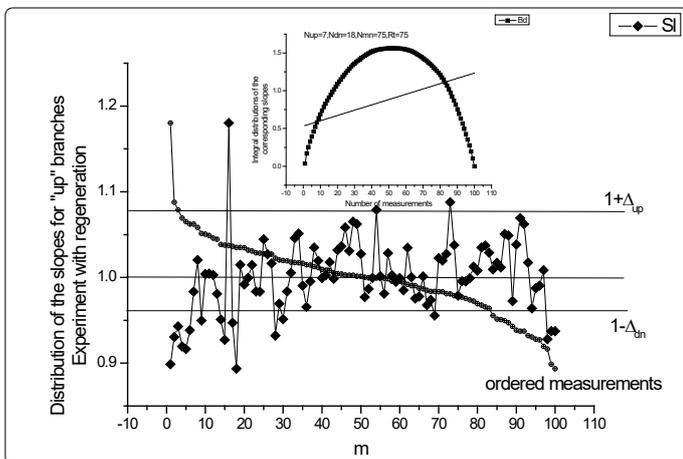

Figure 3c. The distributions of the slopes corresponding to the "up" branches of experiments with regeneration. Number of measurements participating in the averaging procedure and satisfying to the condition
((Nup=7)+(Ndn=18)+(Nmn=75)=(M=100)) and the parameter Rt=75 from (4) are shown in the small figure above.
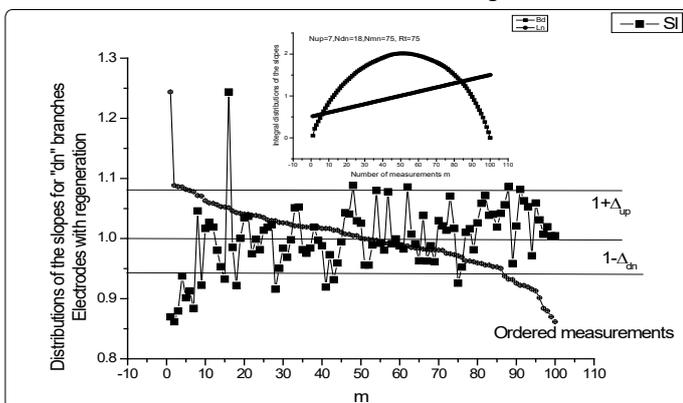

Figure 3d. The distributions of the slopes corresponding to the "dn" branches of experiments with regeneration. Number of measurements participating in the averaging procedure and satisfying to the condition
((Nup=7)+(Ndn=18)+(Nmn=75)=(M=100)) and the parameter Rt=75 from (4) are shown in the small figure above.

So, if this clusterization will be realized then instead of 100 initial measurements we have approximately

$$Yup(x) = \frac{1}{Nup} \sum_{m=1}^{Nup} J_m^{(up)}(x), \ 1 + \Delta_{up} < Sl_m < SL_1,$$

$$Ydn(x) = \frac{1}{Ndn} \sum_{m=1}^{Ndn} J_m^{(dn)}(x), \ SL_M < Sl_m < 1 - \Delta_{dn}, \quad (21)$$

$$Ymn(x) = \frac{1}{Nmn} \sum_{m=0}^{Nmn-1} J_m^{(mn)}(x), \ 1 - \Delta_{dn} < Sl_m < 1 + \Delta_{up}.$$

Here the function Sl_m determines the slopes located in the descending order and the parameters $D_{up,dn}$ associated with the value of the confidence interval is selected for each specific set of measurements *separately*. After realization of this useful procedure one can fit only the mean function $Ymn(x)$. Other two functions $Yup(x)$ and $Ydn(x)$ become strongly-correlated and can be associated with two close curves in accordance with expression (8)

$$Yup(x) = a_1 Ydn(x) + a_0 Ymn(x),$$

$$Yup(x) \equiv J_{tot}(z\xi^2), \ Ydn(x) \equiv J_{tot}(z\xi), \ Ymn(x) \equiv J_{tot}(z) \quad (22)$$

This simple observation allows us to find the unknown constants $a_{1,0}$ from the LLSM and calculated the desired roots from the quadratic equation

$$\kappa^2 - a_1\kappa - a_0 = 0, \ \kappa_i = 1/b_i, \ i = 1, 2. \quad (23)$$

Equation (23) allows restoring also the scaling parameters b_i entering to the percolation channel (2). In equation (22) we have two independent variables x and z. It is necessary to choose the common scale that could be acceptable for the realization of the fitting procedure. If we choose the following values for the down (dn) VAG branch as $LU_{max} = \ln(U_{min}/-1)$ with $U_0 = -1$ and $LU_{min} = \ln(10^{-2})$ and for the "up" branch the variable $LU_{up} = -LU_{dn}$ then in this scale

$$x_j \equiv \ln z_j = LU_{max} + \frac{j}{N}(LU_{min} - LU_{max}), \ j = 1, 2, ..., N, \quad (24)$$

corresponding VAGs remains invariant relatively the chosen number of points. So, this scale as the most convenient is chosen for the fitting purposes.

Stage 2. The Fitting of the Mean Curves Ymn(lnz) to the Function (14)

For realization of the desired fit we normalize these curves to the interval [0,1] that cannot change essentially the essence of the applied approach. As it has been mentioned above, we chose the logarithmic scale (24) where the corresponding VAGs do not change their form. The normalized mean curve for two branches and two experimental situations (without and with electrodes regeneration) are calculates as

$$y(x) = \frac{Ymn(x) - \min(Ymn(x))}{\max(Ymn(x) - \min(Ymn(x)))} + \varepsilon \quad (25)$$

We take the small value of the e = 10^{-6}. These two simple linear transformations realized for the mean curves $Ymn(x)$ allow avoiding some large values of the fitting parameters and

Madridge J Anal Sci Instrum.
ISSN: 2638-1532

Volume 2 • Issue 1 • 1000110

52

uncertainties related the taking of the natural logarithm from zero. The final fit of the normalized curves for all four branches are depicted on Figs.4 (a,b), correspondingly. The additional fitting parameters ($\ln x$, $k_{1,2}$, $n_{1,2}$) and the distributions of the amplitudes $Ac_k^{(1,2)}$, $As_k^{(1,2)}$ (k=1,2,...,K=4) entering into expression (14) for these four normalized branches are collected in Tables 1, 2, correspondingly. So, this theory helps to restore the fractal parameters and partly its discrete structure that characterize the percolation structure of the conducting channels.
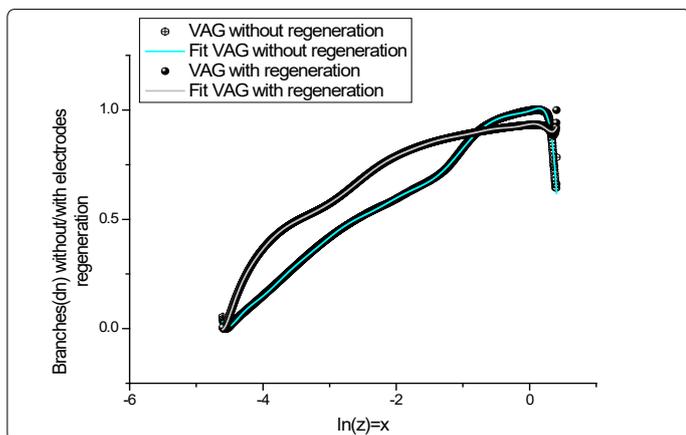

Figure 4a. The fitting of the normalized VAGs with respect to expression (14) for two normalized branches(dn) corresponding to electrodes with/without regeneration. The fitting parameters of these curves are collected in Tables 1 and 2. The influence of regeneration is clearly noticeable.
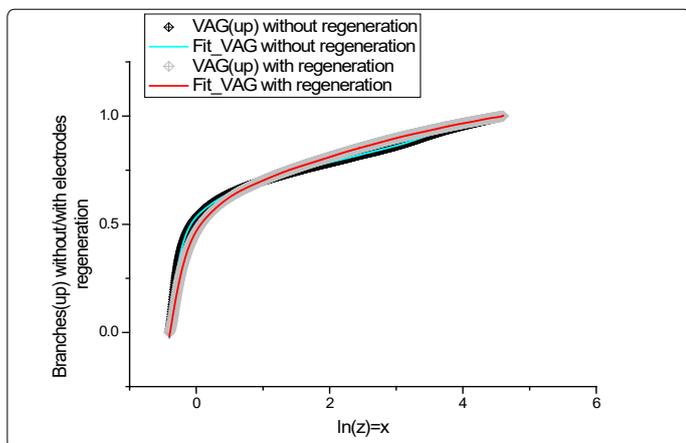

Figure 4b. The fitting of the normalized VAGs with respect to expression (14) for two branches (up) corresponding to electrodes with/without regeneration. The fitting parameters of these curves are collected also in Tables 1 and 2.

Table 1. The additional fitting parameters figuring in the fitting function (14).

The name of the file	$\ln(x)$	k_1	k_2	n_1	n_2	E_0	Rel Err(%)
Branch(dn) without regeneration	-7.20473	1.55397	-0.99921	0.06118	-1.10127E-4	-4853.72	1.15779
Branch(dn) with regeneration	-7.03939	1.75352	-1.00197	0.07978	2.79645E-4	3709.16	0.4818
Branch(up) without regeneration	4.72466	1.86917	-1.00083	-0.13239	-1.74584E-4	-2.61452	0.2215
Branch(up) with regeneration	7.20473	1.53822	-0.9975	-0.05977	3.48023E-4	2541.8	0.19426

Table 2. The distribution of the amplitudes $Ac_k^{(1,2)}$, $As_k^{(1,2)}$ that enter in the fitting function (14) for 4 types of the normalized VAGs. The total number of modes K=4.

The name of the file	$Ac_k^{(1)}$	$As_k^{(1)}$	$Ac_k^{(2)}$	$As_k^{(2)}$
Branch(dn) without regeneration	-8686.56	-3437.28	27198.5	4834.29
	-480.91	-10061.5	-10523.2	12368.5
	3277.03	281.068	-1058.47	-2336.64
	-74.6822	226.427	56.7248	2.59182
Branch(dn) with regeneration	7723.36	2018.34	-21785	-1934.03
	1671.33	7707.55	6226.69	-10706.2
	-2343.98	404.825	1127.61	1448.66
	-0.74759	-158.348	-36.6513	6.87951
Branch(up) without regeneration	1.75014	-0.05769	4.33094	13.7754
	2.94648	-0.66586	-2.14537	-10.1256
	-1.78289	0.5965	0.44001	2.38856
	0.23001	-0.11056	-0.00658	-0.10908
Branch(up) with regeneration	5483.71	1289.13	-15004.2	-1086.73
	1257.89	5495.32	4052.47	-7534.03
	-1684.63	297.719	836.338	962.631
	0.14841	-114.672	-24.8502	7.36171

Stage 3. Reduction to Three Incident Points as the Test of a Possible Self-Similarity

In this subsection we want to suggest a test for detection of self-similar curves that form the measured VAG. Let us choose some interval [x_0, x_{k-1}] containing a set of k data points {(x_0, y_0), ... , (x_{k-1}, y_{k-1}) K=0,1,...,k-1}. One can reduce this information into *three incident points* if the first point is associated with the mean value of the amplitudes and the other two points are associated to their maximal and minimal values, correspondingly. So, this selection represents the simplest reduction of the given set of k randomly selected points to *three* characteristic points p_1=mean{y_0, ... , y_{k-1}}, p_2=max{y_0, ... , y_{k-1}}, p_3=min{y_0, ... , y_{k-1}}. If in the result of this reduction procedure we obtain the curve similar to the initial one then one conclude that obtained three curves are self-similar to the initial curve. This procedure helps to decrease the number of initial points and consider the reduced curves distributed over on the set of "fat" points. R = [N/L], r = 0,1,...,R-1. Here the symbol [..] defines the integer part of the ratio N/K, where N is the total number of points and K is the length of the chosen "cloud" of points. The result of reduction of two "down" initial VAGs and corresponding to electrodes with/without regeneration are shown in Figs. 5(a,b). For R=50, L=24 the self-similarity property is clearly noticeable. The same result is obtained for two self-similar curves corresponding to "up" branches and thereby it is not shown. This simple test serves as an additional argument for selection of the fitting model (14) described above.
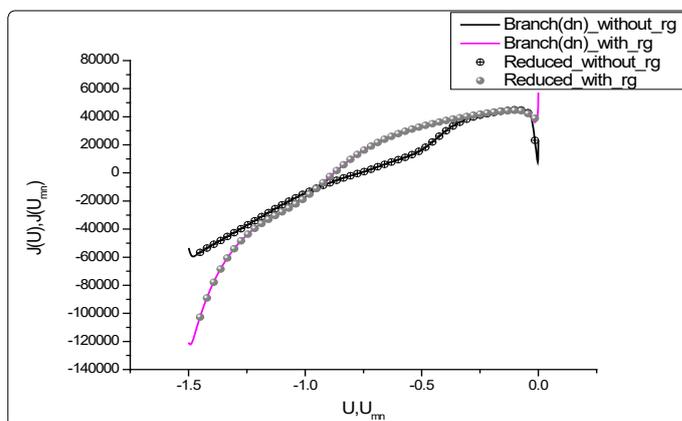

Figure 5a. This figure demonstrates clearly the self-similarity property between initial curve (solid lines) corresponding to down branches and their reduced curves (points). The length of a cloud of points subjected to reduction procedure L=24. Number of "fat" points R=50.

Madridge J Anal Sci Instrum.
ISSN: 2638-1532
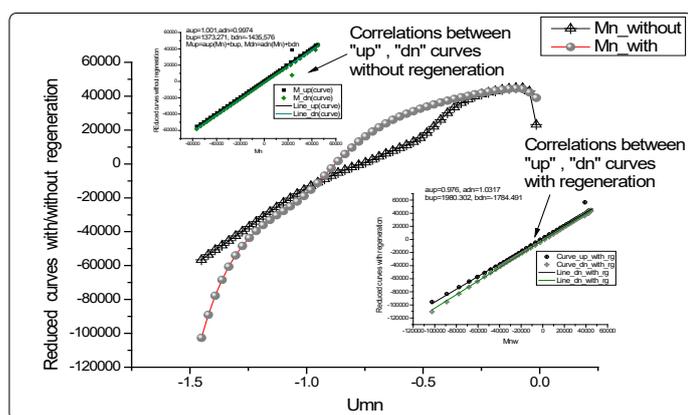
Volume 2 • Issue 1 • 1000110

53

Figure 5b. On the central figure we show the reduced curves corresponding to "down" branches for electrodes with/without regeneration having $R=50$ "fat" points. On the small figures we demonstrate the strong correlations between the mean curve and two curves corresponding to reduction to maximal/minimal points in each section $L=24$ correspondingly.

Conclusion

May be this theory is not complete but it reflects the influence of existing fractal structure of the measured electrodes and conducting media that take place during the electrochemical process. We believe that this theory can find its wide application for quantitative description of a various VAGs. In particular, in solutions of electroanalysis problems associated with in detection of possible traces of the solute substances, when the peaks of oxidation\restoration potentials are close to each other. This phenomenon is observed in analysis of VAGs associated with optically active compounds as *enantiomers*, having practical importance in medicine. From practical point of view, the suggested quantitative method one can apply for evaluation of the effectiveness of the medical drug and identify one enantiomer (the micro component of the medical drag with negative reaction to the human's body) and in its abundance, when it has a positive influence. In this case, the total background current will coincide with current of the given solute mixed with current belonging to macro-component. The detection of the micro-component current one can evaluate quantitatively analyzing, in turn, the measured VAG based on the approach suggested above. But the additional and justified arguments tested on a wide experimental material need a further research.

Mathematical Appendix

In this Appendix we want to justify the common selection of the scaling parameter x that enters in the general fitting formula (12). Let us suppose that instead of the scaling factor x^n we have the product $\xi_1\xi_2...\xi_n$ generated by the random structure of the percolation cluster. We suppose also that these random scaling factors have small deviations relatively the mean value $\xi_i = \langle\xi\rangle + \delta_i$, $|\delta_i| << \langle\xi\rangle$. If we put these factors into the product we obtain

$$\prod_{i=1}^{n}\xi_i = \exp\left[\left(\sum_{i=1}^{n}\ln\left(\langle\xi\rangle+\delta_i\right)\right)\right] = \langle\xi\rangle^n \exp\left[\left(\sum_{i=1}^{n}\ln\left(1+\frac{\delta_i}{\langle\xi\rangle}\right)\right)\right]$$

$$\cong \langle\xi\rangle^n \exp\left(\frac{\langle\delta\rangle}{\langle\xi\rangle} - \frac{1}{2}\frac{\langle\delta^2\rangle}{\langle\xi\rangle^2} + ...\right)^n, \ \langle\delta^s\rangle = \frac{1}{n}\sum_{i=1}^{n}(\delta_i)^s.$$

(A1)

This useful relationship shows that it is possible to replace the set of the random scaling parameters by one averaged parameter in accordance with the relationship

$$\xi \to \langle\xi\rangle \exp\left(\frac{\langle\delta\rangle}{\langle\xi\rangle} - \frac{1}{2}\frac{\langle\delta^2\rangle}{\langle\xi\rangle^2} + ...\right)$$

(A2)

Therefore in the main text we imply this parameter in the *averaged* sense, which is evaluated with the help of the fitting procedure.

Acknowledgement

References

1. Eksperiandova LP, Belikov KN, Khimchenko SV, Blank TA. Once again about determination and detection limits. *J. Anal. Chem.* 2010; 65(3): 223-228. doi: 10.1134/S1061934810030020

2. Otto M. Analytische Chemi. Weinheim: Wiley-VCH; Fourth edition, 2011.

3. Scholz F (Ed.) Electroanalytical Methods, Guide to Experiments and Applications. Springer-Verlag Berlin Heidelberg. 2002.

4. Pomerantsev AL. Chemometrics in Excel. New York: *Wiley Online Library*. 2014; doi: 10.1002/9781118873212

5. Winquist F, Wide P, Lundstrom L. An electronic tongue based on voltammetry. *Anal. Chim. Acta.* 1997; 357(1-2): 21-31. doi: 10.1016/S0003-2670(97)00498-4

6. Henze G. Polarographie und Voltammetrie. Springer-Verlag Berlin Heidelberg. 2001.

7. Compton RG, Banks CE. Understanding voltammetry: Second edition. Imperial College Press. 2011.

8. Hamann CH, Vielstich W. Elektrochemie, Bd. I u. II aus der Reihe „taschentext".Weinheim: Verlag Chemie. 1975.

9. Schwabe K. Physikalische Chemie, Bd. 2, Elektrochemie. Akademie-Verlag Berlin. 1986.

10. Winquist F. Voltammetric electronic tongues – basic principles and applications. *Microchim. Acta.* 2008; 163(1-2): 3-10. doi: 10.1007/s00604-007-0929-2

11. Winquist F, Olsson J, Eriksson M. Multicomponent analysis of drinking water by a voltammetric electronic tongue. *Anal. Chim. Acta.* 2011; 683(2): 192-197. doi: 10.1016/j.aca.2010.10.027.

12. Ruiz GA, Felice CJ. Electrochemical-fractal model versus randles model: A discussion about diffusion process. *Int. J. Electrochem. Sci.* 2015; 10(10): 8484-8496

13. Anastopoulos AG, Bozatzidis AI. Detection of the fractal character of compact adsorbed layers by the dropping mercury electrode. *Electrochim. Acta.* 2009; 54(16): 4099-4104. doi: 10.1016/j.electacta.2009.02.042

14. Felice CJ, Ruiz GA. Differential equation of a fractal electrode–electrolyte interface. *Chaos, Solitons and Fractals.* 2016; 84: 81-87. doi: 10.1016/j.chaos.2016.01.003

15. Fernández-Martínez M, Nowak M, Sánchez-Granero MA. Counterexamples in theory of fractal dimension for fractal structures. *Chaos, Solitons and Fractals.* 2016; 89: 210-223. doi: 10.1016/j.chaos.2015.10.032

16. Mayrhofer-Reinhartshuber M, Ahamme H. Pyramidal fractal dimension for high resolution images. *Chaos.* 2016; 26 (7): 1-7. doi: 10.1063/1.4958709

17. Kant PR. General Theory for Pulse Voltammetric Techniques on Rough and Finite Fractal Electrodes for Reversible Redox System with Unequal Diffusivities. *Electrochim. Acta.* 2016; 194: 283-291. doi: 10.1016/j.electacta.2016.02.039

Madridge J Anal Sci Instrum.
ISSN: 2638-1532

Volume 2 • Issue 1 • 1000110

54

18. Nigmatullin RR, Budnikov HC, Sidelnikov AV. New Approach for Voltammetry Near Limit of Detection: Integrated Voltammograms and Reduction of Measurements to an "Ideal" Experiment. *Electroanalysis.* 2015; 27(6): 1416-1426. doi: 10.1002/elan.201400735

19. Nigmatullin RR. Recognition of nonextensive statistical distributions by the eigencoordinates method. *Physica A.* 2000; 285(3-4): 547-565. doi: 10.1016/S0378-4371(00)00237-5

20. Nigmatullin RR, Le Mehaute A. Is there geometrical/physical meaning of the fractional integral with complex exponent? *J. Non-Cryst. Solids.* 2005; 351(33-36): 2888-2899. doi: 10.1016/j.jnoncrysol.2005.05.035

21. Nigmatullin RR, Machado JT, Menezes R. Self-similarity principle: the reduced description of randomness. *Central European Journal of Physics.* 2013; 11(6): 724-739. doi: 10.2478/s11534-013-0181-9

22. Nigmatullin RR, Baleanu D. New relationships connecting a class of fractal objects and fractional integrals in space. *Fractional Calculus and Applied Analysis.* 2013; 16(4): 911-936. doi: 10.2478/s13540-013-0056-1

Madridge J Anal Sci Instrum.
ISSN: 2638-1532

Volume 2 • Issue 1 • 1000110

55